Entanglement preparation and nonreciprocal excitation evolution in giant atoms by controllable dissipation and coupling

Hongwei Yu, Zhihai Wang,* and Jin-Hui Wu
Center for Quantum Sciences and School of Physics, Northeast Normal University, Changchun 130024, China

(Received 4 January 2021; revised 7 April 2021; accepted 12 July 2021; published 21 July 2021)

We investigate the dynamics of a giant atom (or atoms) in a waveguide QED scenario, where the atom couples to the coupled resonator waveguide via two sites. For a single-giant-atom setup, we find that the atomic dissipation rate can be adjusted by tuning its size. For the two-giant-atom system, the waveguide will induce the controllable individual and collective dissipation as well as effective interatom coupling. As a result, we can realize theoretically the robust entangled state preparation and nonreciprocal excitation evolution. We hope our study can be applied in quantum information processing based on a photonic and acoustic waveguide setup.

DOI: 10.1103/PhysRevA.104.013720

I. INTRODUCTION

The giant atom, which can be realized by superconducting qubits (artificial atoms), is a new component in the field of quantum optics [1]. Since the size of the giant atom can be comparable to the wavelength of light, the traditional dipole approximation breaks down in the light-atom interaction. As a result, the giant atom is nonlocally coupled to the waveguide via multiple connecting points and the interference effect between these points will dramatically modulate the collective behavior of the atoms. In this community, the mutual control between the photon and atom has been attracting increasing attention both theoretically and experimentally [2–11].

The coupled resonator waveguide (CRW) has been widely studied in a photon-based quantum network [12]. On the one hand, it supplies a channel for the traveling photon with tunable group velocity, and the single- [13,14] or few-photon scattering [15,16] has been used to construct the photon device, such as a quantum transistor [17], router [18], and frequency converter [19]. On the other hand, due to its exotic energy band, the CRW provides a structured environment for the atom to form the atom-photon dressed state and control the dissipation or decoherence of the atom [20]. Meanwhile, as a data bus, the CRW can also induce the effective coupling between remote atoms [21–23] and is therefore widely used in quantum information processing.

In the giant-atom–CRW coupled system, we have shown that the size of the giant atom can serve as a sensitive controller to regulate the single-photon transmission and photonic bound state in the waveguide [24]. The further question is how to control the dissipation and indirect interaction between the giant atoms by their own size when being subject to the environment which consists of the CRW.

To tackle this issue, we first consider a system consisting of a single giant atom, which couples to a CRW via two distant sites. Within the Born-Markovian approximation, we show that the dissipation rate of the giant atom can be equal to or smaller than that of a conventional small atom or even surprisingly achieves zero, depending on the size of the atom. It is then generalized to the system consisting of two giant atoms. We find that the collective decoherence and effective interaction are accompanied by an individual dissipation and all of these processes are finely controllable. By making all of the waveguide-induced dissipation zero, we propose a robust scheme to realize the entanglement preparation. More interestingly, when only the collective dissipation is suppressed, we can realize a parity-time ($\mathcal{PT}$)-like symmetry and nonreciprocal excitation evolution for a fixed giant atom. However, the excitation transmission between them is reciprocal, which is dramatically different from that in the quantum system with time-reversal symmetry broken [25–28].

The rest of the paper is organized as follows. In Sec. II we present the single-giant-atom model and discuss its controllable dissipation due to the coupling to the waveguide. In Sec. III we generalize to the two-atom setup and investigate the applications in entangled state preparation and nonreciprocal excitation evolution. In Sec. IV we provide a short summary and discussion.

II. CONTROLLABLE DISSIPATION FOR A SINGLE GIANT ATOM

As sketched in Fig. 1(a), the system we consider consists of an array of an $N_c \to \infty$ coupled-resonator waveguide and a two-level system. Here we consider a giant-atom scenario, where the two-level system couples to the waveguide via two sites. In what follows we refer to such a two-level system as a giant atom. The atom-waveguide coupled system considered can be realized in superconducting quantum circuits, which is demonstrated in Fig. 1(b). Here the *LC* circuits (LCCs) serve as the resonators and the transmon qubit serves as the two-level system, that is, the giant atom. The capacities couple the resonators as well as the resonators and the transmon. The

*wangzh761@nenu.edu.cn

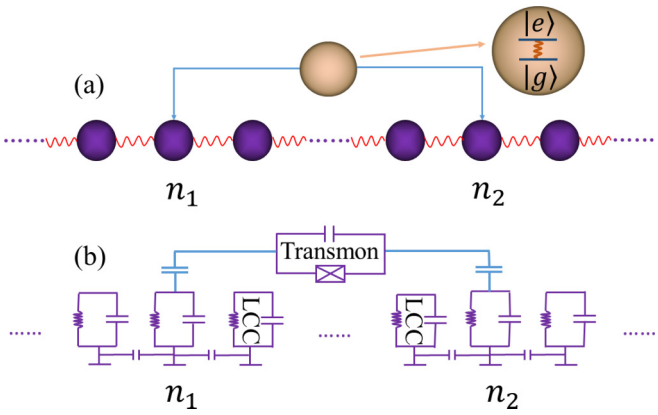

FIG. 1. (a) Sketch of the waveguide QED setup, where a giant atom is coupled to a photonic lattice via the n_1th and n_2th sites. (b) Effective circuit diagram of the device.

Hamiltonian of the system is written as $H = H_c + H_I$, where ($\hbar = 1$)

$$H_c = \omega_c \sum_j a_j^\dagger a_j - \xi \sum_j (a_{j+1}^\dagger a_j + a_j^\dagger a_{j+1}), \tag{1}$$

$$H_I = \Omega |e\rangle\langle e| + g\left[\left(a_{n_1}^\dagger + a_{n_2}^\dagger\right)\sigma^- + \text{H.c.}\right]. \tag{2}$$

Here ω_c is the frequency of the resonators, a_j is the bosonic annihilation operator on site j, ξ is the hopping strength between the nearest resonators, $\sigma^\pm$ are the usual Pauli operators of the giant atom, and Ω is the transition frequency of the giant atom between the ground state $|g\rangle$ and the excited state $|e\rangle$. We have considered that the giant atom couples to the waveguide via the n_1th and n_2th resonators with coupling strength g. We have performed the rotating-wave approximation in the interresonator and atom-waveguide coupling Hamiltonian.

Introducing the Fourier transformation $a_j = \sum_k a_k e^{ikj}/\sqrt{N_c}$, the Hamiltonian of the waveguide H_c can be written in a diagonal form $H_c = \sum_k \omega_k a_k^\dagger a_k$, where the dispersion relation is given by $\omega_k = \omega_c - 2\xi \cos k$. The waveguide therefore supports a single-photon continual band which is centered at ω_c with a width of 4ξ. In this sense, the waveguide supplies a structured environment for the giant atom. When the giant atom is outside the waveguide in the frequency domain, the dissipation will be suppressed due to the dispersive coupling to the waveguide. In contrast, when the transition frequency of the giant atom is located inside the waveguide and far away from the upper and lower edges of the band, the initial excited atom will undergo an exponential decay in population. In this sense, the frequency of the giant atom can be used to control its dissipation dynamics via the trivial resonant mechanism. However, we will show here that the interference effect induced by the intrinsic character of the giant atom makes its size another controller, even when the atomic frequency is inside the energy band of the waveguide, for example, when the giant atom is resonant with the bare resonator in the waveguide.

To obtain the master equation for the density matrix of the giant atom, we work in the momentum representation and interaction picture. Then the atom-waveguide coupling Hamiltonian is expressed as [20]

$$H_I(t) = g \sum_{i=1}^{2} [\sigma^+ E(n_i, t) e^{i\Omega t} + \sigma^- E^\dagger(n_i, t) e^{-i\Omega t}], \tag{3}$$

where $E(n_i, t) = \frac{1}{\sqrt{N_c}} \sum_k (e^{-i\omega_k t} e^{ikn_i} a_k)$. With the Born-Markovian approximation, the master equation is formally written as [29]

$$\dot{\rho}(t) = -\int_0^\infty d\tau \, \text{Tr}_c\{[H_I(t), [H_I(t-\tau), \rho_c \otimes \rho(t)]]\}. \tag{4}$$

In what follows we will consider that the giant atom is resonant with the bare resonator, that is, $\Omega = \omega_c$. In this situation, after some direct calculations as shown in Appendix A, the master equation is finally simplified as

$$\dot{\rho} = -i\Omega[|e\rangle\langle e|, \rho] + (A + A^*)\sigma^- \rho \sigma^+ - A\sigma^+\sigma^- \rho - A^* \rho \sigma^+ \sigma^-, \tag{5}$$

where

$$A = \frac{g^2}{\xi}(1 + e^{i\pi N/2}), \tag{6}$$

with $N = |n_1 - n_2|$ characterizing the size of the giant atom, that is, the distance between the two-atom–CRW connecting points.

This shows that the dissipation of the giant atom can be tuned on demand by changing its size. For example, when $N = 4m + 2$ with integral $m = 0, 1, 2, \ldots$, the dissipation rate is $A = 0$, which implies that the atom will not undergo dissipation and decoherence. Therefore, we can realize a decoherence protection via a giant-atom setup even when it is located inside the waveguide in energy and this protection is not possible in a traditional small-atom scheme, which interacts with only one site. On the other hand, when $N = 4(m + 1)$, the dissipation rate of the giant atom becomes $J = 2g^2/\xi$, which is the same as that in the small-atom setup when the atom-waveguide coupling strength is $2g$. Finally, when the size of the giant atom satisfies $N = 2m + 1$, $A = g^2(1 \pm i)/\xi$ becomes a complex number, with the real part representing the decay rate $J_0 = J/2$ and the imaginary part $\delta_0 = \pm J_0$ representing the atom-waveguide coupling inducing frequency shift. In the typical waveguide system consisting of superconducting circuits, where the interresonator coupling strength can be achieved by $\xi/2\pi = 100$ MHz [30], it is easy to work in the parameter regime of $\delta_0 \ll |2\xi|$, where the modified frequency of the giant atom is still inside the single-photon band of the waveguide and we can still describe the dynamics of the atom via the master equation (5).

The underlying physics in the above discussion is that the waveguide serves as a structured environment, which induces the dissipation of the giant atom. As a result, the evolution of the excited-state population yields

$$P_e(t) = |\langle |e\rangle\langle e| \rangle| = e^{-2\,\text{Re}(A)t} \tag{7}$$

for the initial excited giant atom.

For $N = 3$ and 4 where $\text{Re}(A) \neq 0$, we plot the curve of $P_e(t)$ by neglecting the small atomic intrinsic dissipation in Fig. 2(a). Here the solid lines are the approximate results obtained by Eq. (7) and the dashed lines are the numerical results

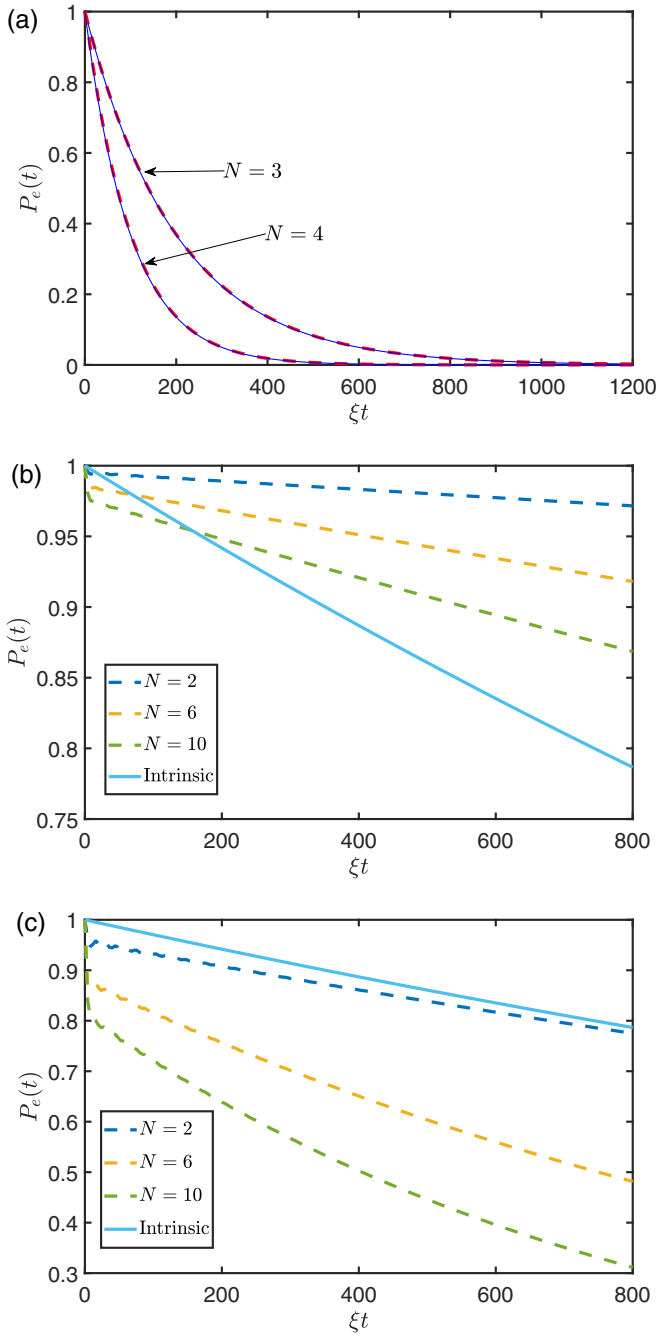

FIG. 2. Evolution of the excited-state population $P_e(t)$. The dashed and solid lines in (a) are the approximate analytic results in Eq. (7) and the exact numerical results, respectively (see Appendix B). The parameters are $\Omega = \omega_c$, $N_c = 4000$, $\kappa/\xi = 6 \times 10^{-3}$, and (a) and (b) $g/\xi = 0.05$ and (c) $g/\xi = 0.15$. The intrinsic decay rate for the giant atom is taken as $\gamma_1/\xi = 3 \times 10^{-4}$ in (b) and (c).

obtained by including a small loss rate κ for each resonator (see Appendix B for a detailed description of the numerical calculations). The results in Fig. 2(a) show good agreement between the approximate and the numerical treatment for the atom-waveguide coupling strength $g = 0.05\xi$. Furthermore, Eq. (7) implies that $P_e(t) = e^{-2g^2t/\xi}$ for $N = 3$ and $P_e(t) = e^{-4g^2t/\xi}$ for $N = 4$. Therefore, the atom for $N = 4$ decays faster than that for $N = 3$, which is also clearly demonstrated in Fig. 2(a). Our further simulations (not shown here) show that Eq. (7) works well even when the atom-waveguide coupling strength achieves $g/\xi = 0.2$, below which the numerical result is nearly independent of N.

On the other hand, for $N = 2, 6, 10, \ldots$, the Markovian master equation (5) with (6) tells us the atom will not decay by coupling to the waveguide channel. Thus, the main dissipation comes from intrinsic decay, which is induced by the coupling to the surrounding environment except the waveguide. Then the population yields $P_e(t) = e^{-\gamma_1 t}$, where γ_1 is the intrinsic decay rate. It is therefore necessary to investigate when the high-order non-Markovian effects will dominate the intrinsic decay. To this end, we show the full numerical dynamics for the above N in Figs. 2(b) and 2(c) as well as the dynamics with only the intrinsic dissipation for comparison. Here the dashed lines are the results obtained by omitting the intrinsic decay, that is, the giant atom does not couple to the other environments except for the waveguide. The solid lines are the results obtained by considering only the intrinsic decay, but without that induced by the waveguide channel. It is obvious that the numerical dynamics (dashed lines) depends dramatically on N and the excited-state population decay becomes faster as N increases. For a weak atom-waveguide coupling strength ($g/\xi = 0.05$) in Fig. 2(b), the decay induced by the waveguide channel for $N = 2, 6, 10$ is dominated by the intrinsic decay on a long timescale with $\gamma_1/\xi = 3 \times 10^{-4}$, that is, the dashed lines are above the solid lines. By increasing g while fixing γ_1, we show in Fig. 2(c) that the waveguide-channel-induced decay will surpass intrinsic decay even for $N = 2$, which is the smallest value allowed by $A = 0$, for $g/\xi = 0.15$. In this situation, the high-order or non-Markovian effect becomes more important than the error source intrinsic to the giant atom and the dashed lines are below the solid lines.

III. TWO-GIANT-ATOM SETUP

To explore the potential application of the giant atom in the quantum information processing, we generalize the above discussion to the setup consisting of two giant atoms. Then the total Hamiltonian for the system is

$$H_2 = H_c + \Omega(|e\rangle_1\langle e| + |e\rangle_2\langle e|) + g(a^\dagger_{n_1}\sigma_1^- + a^\dagger_{n_2}\sigma_1^- + \text{H.c.}) + g(a^\dagger_{m_1}\sigma_2^- + a^\dagger_{m_2}\sigma_2^- + \text{H.c.}), \tag{8}$$

which implies that the first atom couples to the waveguide at the n_1th and n_2th sites, while the second atom couples to the waveguide at the m_1th and m_2th sites. Similar to the treatment for the single giant atom, we can obtain the master equation as

$$\dot{\rho} = -i[\mathcal{H}, \rho] + \sum_{i,j=1}^{2} \frac{\Gamma_{ij}}{2}(2\sigma_j^-\rho\sigma_i^+ - \sigma_i^+\sigma_j^-\rho - \rho\sigma_i^+\sigma_j^-), \tag{9}$$

where the coherent coupling between the two atoms is described by the Hamiltonian

$$\mathcal{H} = \sum_{i=1}^{2}\left(\Omega + \frac{U_{ii}}{2}\right)|e\rangle_i\langle e| + \frac{U_{12}}{2}(\sigma_1^+\sigma_2^- + \text{H.c.}). \tag{10}$$

In the above equations, we have defined $U_{ij} := 2\,\mathrm{Im}(A_{ij})$ and $\Gamma_{ij} := 2\,\mathrm{Re}(A_{ij})$; in addition,

$$A_{11} = \frac{g^2}{\xi}(1 + e^{i(\pi/2)|n_1 - n_2|}), \tag{11a}$$

$$A_{22} = \frac{g^2}{\xi}(1 + e^{i(\pi/2)|m_1 - m_2|}), \tag{11b}$$

$$A_{12} = A_{21} = \frac{g^2}{2\xi}\sum_{i,j=1}^{2} e^{i(\pi/2)|n_i - m_j|}. \tag{11c}$$

This shows that the individual dissipation rate (Γ_{11} and Γ_{22}) and frequency shift (U_{11} and U_{22}) of the two giant atoms are determined by the size of each giant atom. Furthermore, the waveguide can also serve as a data bus to induce the interaction and collective dissipation between two giant atoms, for which the rates are given by U_{12} and Γ_{12}, respectively. They are determined by both the size of the two giant atoms and their relative locations. Taking advantage of the tunable nature of A_{ij} by the formulation of the giant atom, we will show two applications in quantum information processing in what follows.

A. Entangled state preparation

As the first application, we discuss the entangled state preparation. We can appropriately choose n_1, n_2, m_1, and m_2 such that $\Gamma_{11} = \Gamma_{22} = U_{11} = U_{22} = \Gamma_{12} = 0$ and $U_{12} = 2J = 4g^2/\xi$ are satisfied. In this situation, the waveguide will only induce the interaction between the two giant atoms. As a result, the master equation in the rotating frame defined by the free term of atoms is reduced to $\dot{\rho} = -i[H_0, \rho]$, with

$$H_0 = J(\sigma_1^+\sigma_2^- + \sigma_2^+\sigma_1^-). \tag{12}$$

The initial state is prepared as $|\psi(0)\rangle = |e; g\rangle$, which represents that the first atom is in the excited state while the second one is in the ground state. At an arbitrary moment t, the wave function of two-giant-atom system becomes

$$|\psi\rangle = \cos(Jt)|e; g\rangle - i\sin(Jt)|g; e\rangle. \tag{13}$$

Choosing the evolution time $t = \pi/(4J)$, we can achieve the maximum entangled state $|\psi\rangle = (|e; g\rangle - i|g; e\rangle)/\sqrt{2}$.

In the above entangled state preparation scheme, we have only considered the effect of the waveguide. In fact, the atoms also inevitably interact with the external environment. In such a case, the dynamics of the system is governed by the master equation

$$\dot{\rho} = -i[H_0, \rho] + \frac{\gamma_1}{2}\sum_{i=1}^{2}(2\sigma_i^-\rho\sigma_i^+ - \sigma_i^+\sigma_i^-\rho - \rho\sigma_i^+\sigma_i^-) + \frac{\gamma_2}{2}\left(\sigma_1^z\rho\sigma_1^z + \sigma_2^z\rho\sigma_2^z - 2\rho\right). \tag{14}$$

Here the first line represents the unitary evolution mediated by the waveguide and the dissipation or decoherence process with rate γ_1, which is the same as that in the preceding section. The second line represents the pure dephasing process with rate γ_2.

In superconducting circuits, the LCCs serve as the resonators and the transmon serves as the giant atom. In recent experiments, the coupling strength between the nearest LCCs can be achieved by $\xi/2\pi = 100$ MHz [30] and the light-matter interaction has been achieved in the ultrastrong-coupling and deep strong-coupling regimes in the superconducting circuit QED system [31,32]. The transition frequency of the giant atom and the eigenfrequency of the LCCs are both on the order of several gigahertz and the atom-waveguide coupling strength easily achieves the order of megahertz, so the waveguide inducing an atom-atom coupling strength $J = 2g^2/\xi$ is on the order of megahertz. Moreover, the intrinsic decoherence time of the superconducting qubit (for example, the transmon) is achieved by $T_1 = 20\ \mu$s and $T_2^* = 10\ \mu$s [33] or even longer [34], which implies that $\gamma_1/2\pi \leqslant 8$ kHz and $\gamma_2/2\pi \leqslant 16$ kHz, that is, γ_1/J and γ_2/J are on the order of 10^{-3}–10^{-2}. In Fig. 3(a) we plot the fidelity as a function of γ_1 and γ_2 based on the above master equation. It shows that, even for $\gamma_1 = 0.1J$ and $\gamma_2 = 0.2J$, the fidelity is still higher than 92%.

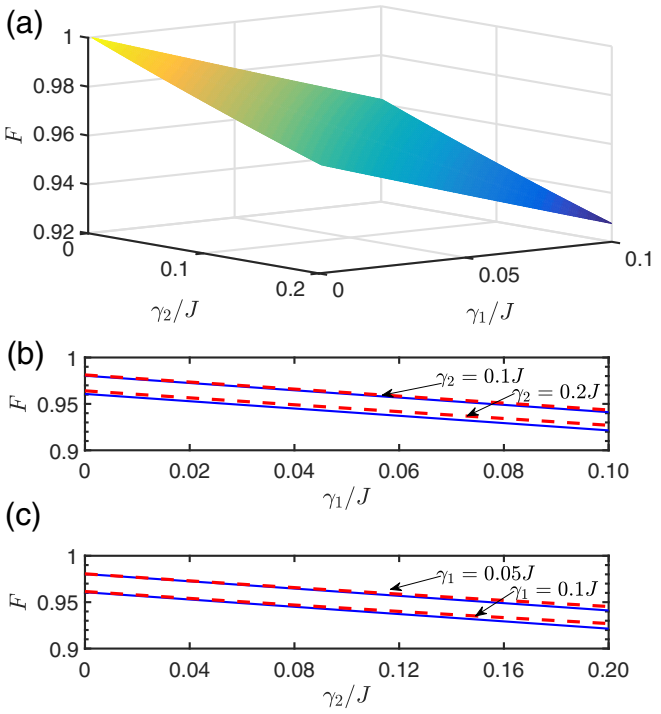

FIG. 3. Fidelity of entangled state preparation: (a) fidelity based on the master equation and (b) and (c) fidelity as a function of γ_1 (γ_2) for different γ_2 (γ_1), where γ_1 and γ_2 are given in units of J.

In our consideration, the effect of the external environment is much smaller than that induced by the waveguide, that is, $(\gamma_1, \gamma_2) \ll J$. Up to the first order of γ_1/J and γ_2/J, the fidelity for the entangled state preparation is approximated as

$$F = \sqrt{\langle\psi|\rho\left(t = \frac{\pi}{4J}\right)|\psi\rangle} \approx 1 - \frac{\pi}{8J}\gamma_1 - \frac{\pi}{16J}\gamma_2. \tag{15}$$

This shows that the coupling to the external environment is harmful for the entangled state preparation in our system and the decoherence process dominates the pure dephasing process in decreasing the fidelity. In Figs. 3(b) and 3(c) we compare the fidelity obtained from the master equation (solid lines) and that from the approximated expression (dashed

lines) in Eq. (15). The fidelity shows a linear dependence on γ_1 as well as γ_2, and the agreement between them implies the validity of Eq. (15).

In the above discussion we have chosen the fixed geometry configuration for the giant atoms, that is, the fixed size for each giant atom and the distance between them. In such a situation, the waveguide only induces the effective interaction between the two giant atoms, but without dissipation. One may also investigate the steady-state entanglement by including a continuous weak driving laser such that the entanglement will show an oscillatory dependence on the size of the giant atoms and the distance between them. The underlying physics is similar to that of the two-small-atom setup [21]. However, such driven-dissipation induced entanglement is beyond the discussion in this work.

B. Nonreciprocal excitation evolution

Next, let us discuss the application in demonstrating the $\mathcal{PT}$-like symmetry physics and nonreciprocal excitation evolution. In contrast to the entangled state preparation scheme, here we set $U_{11} = U_{22} = \Gamma_{12} = 0$ and $U_{12} = 2J$, that is, the two atoms effectively interact with each other and undergo individual dissipations. The dynamics is then governed by the master equation (in the rotating frame)

$$\dot{\rho} = -i[H_0, \rho] + \frac{\Gamma_{11}}{2}(2\sigma_1^- \rho \sigma_1^+ - \sigma_1^+ \sigma_1^- \rho - \rho \sigma_1^+ \sigma_1^-) + \frac{\Gamma_{22}}{2}(2\sigma_2^- \rho \sigma_2^+ - \sigma_2^+ \sigma_2^- \rho - \rho \sigma_2^+ \sigma_2^-), \tag{16}$$

where the Hamiltonian H_0 is given in Eq. (12).

We now consider that only one atom is excited initially and explore the evolution of the excited probability at the same atom. When the initial excitation is at the first atom, that is, $|\psi_1(0)\rangle = |e; g\rangle$, the excited probability is obtained as

$$P_1(t) = \mathrm{Tr}[|e\rangle_1\langle e|\rho_1(t)] = \frac{e^{-\delta t/2}}{2K}[(\Delta^2 - 8J^2)M_+(t) + \sqrt{K}\Delta M_-(t) - 16J^2], \tag{17}$$

where $\rho_1(t)$ is the density matrix at time t, $\delta = \Gamma_{11} + \Gamma_{22}$, $\Delta = \Gamma_{11} - \Gamma_{22}$, and

$$K = \Delta^2 - 16J^2, \tag{18}$$

$$M_\pm(t) = e^{-\sqrt{K}t/2} \pm e^{\sqrt{K}t/2}. \tag{19}$$

It immediately follows that the excited probability decays with time due to the dissipation of the two atoms. However, the decay behavior is also dependent on the competition between the dissipation and coupling. For the situation of $|\Delta| < 4J$, $P_1(t)$ will undergo a small oscillation during the decay, while the oscillation will disappear as $|\Delta| > 4J$; the different behaviors can be observed clearly in Fig. 4(a), where the dynamical evolution of the population is plotted for different Γ_{11} and Γ_{22}. The change from the oscillation decay to nonoscillation decay can be physically explained by the $\mathcal{PT}$-like symmetry phase transition. To understand it intuitively, we describe the system by the non-Hermitian Hamiltonian phenomenologically by neglecting the jump term in the master equation [Eq. (16)]. In this sense, the effective Hamiltonian which governs the dynamics can be written as

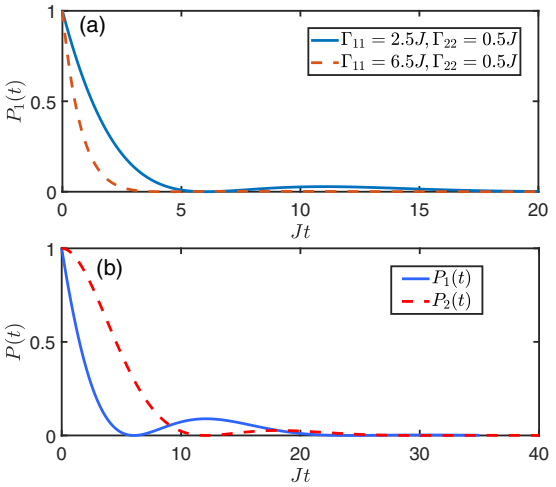

FIG. 4. (a) Trapping population $P_1(t)$. (b) Demonstration of nonreciprocal excitation trapping. The parameters for (b) are $\Gamma_{11} = 0$ and $\Gamma_{22} = 2J$.

$$H_{\mathrm{eff}} = J(\sigma_1^+ \sigma_2^- + \sigma_2^+ \sigma_1^-) - \frac{i\Gamma_{11}}{2}|e\rangle_1\langle e| - \frac{i\Gamma_{22}}{2}|e\rangle_2\langle e|. \tag{20}$$

In the single-excitation subspace, the eigenfrequencies are

$$\omega_\pm = -i\frac{\delta}{4} \pm \frac{\sqrt{-K}}{4}. \tag{21}$$

This shows that the system will undergo a $\mathcal{PT}$-like phase transition as K moves from a negative value to a positive value. In the $\mathcal{PT}$-like symmetry phase with $K < 0$ ($|\Delta| < 4J$), the imaginary parts of $\omega_\pm$ coincide but the real parts differ, with $M_+ \sim \cos(\alpha t/2)$ and $M_- \sim \sin(\alpha t/2)$ for $\alpha = \sqrt{|K|}$. As a result, the dynamics shows an oscillation. In the $\mathcal{PT}$-like symmetry-broken phase with $K > 0$ ($|\Delta| > 4J$), the real parts of $\omega_\pm$ disappear and the imaginary parts differ, with $M_+ \sim \cosh(\alpha t/2)$ and $M_- \sim \sinh(\alpha t/2)$, corresponding to a pure decay dynamical behavior.

We would like to point that, in our scheme, the atom is resonant with the resonators in the waveguide; therefore, the size of each giant atom and the relative location between them make it possible to control the effective interaction and collective or individual dissipation. In the experiments based on a superconducting qubit, the nonlocal coupling between the giant atom and the transmission line can be realized by the capacitance, and two or even more coupling points have been achieved so far [10,11]. On the other hand, the previous calculations show that Γ_{11} and Γ_{22} can only be taken as 0 or $2J$, so the nonzero Δ only yields $|\Delta| = 2J < 4J$. That is, we can only work in the $\mathcal{PT}$-like symmetry phase and observe the oscillation decay in our system. Meanwhile, we have used the non-Hermitian Hamiltonian H_{eff} to analyze $\mathcal{PT}$-like phase transition physics from the viewpoint of the eigenfrequency. As for the dynamics, the non-Hermitian Hamiltonian only works well in the single-excitation subspace, which implies that the jump term in the master equation will not have an effect. However, this is not the case for multiple excitations. For example, when the initial state is prepared as $|\psi(0)\rangle = |e; e\rangle$,

the correct dynamics behavior can be given by the master equation but not $H_{\rm eff}$, because the trace preservation is broken by the non-Hermitian terms.

We now consider that the second atom is initially excited with $|\psi_2(0)\rangle = |g;e\rangle$. Then the excitation probability for the same atom becomes

$$P_2(t) = \mathrm{Tr}[|e\rangle_2\langle e|\rho_2(t)] = \frac{e^{-\delta t/2}}{2K^2}[(\Delta^2 - 8J^2)M_+(t) - \sqrt{K}\Delta M_-(t) - 16J^2], \tag{22}$$

where $\rho_2(t)$ is the density matrix.

We plot the comparison between $P_1(t)$ and $P_2(t)$ in Fig. 4(b) for the parameters used in our giant-atom scheme. It clearly shows a nonreciprocal evolution in that $P_1(t) \neq P_2(t)$. This fact can also be observed by the different signs before the second term of the second lines in Eqs. (17) and (22). This implies that the different decay rates of the two atoms lead to nonreciprocal excitation evolution.

Interestingly, and dramatically different from the unidirectional transmission in most of the $\mathcal{PT}$-symmetric system [27,28], here we observe a reciprocal excitation transmission, that is,

$$T = \mathrm{Tr}[|e\rangle_2\langle e|\rho_1(t)] = \mathrm{Tr}[|e\rangle_1\langle e|\rho_2(t)] = \frac{4J^2}{K}e^{-\delta t/2}(e^{Kt/2} + e^{-Kt/2} - 2). \tag{23}$$

It is obvious that the excitation transmission rate T depends on K via Δ^2, but the excitation populations $P_1(t)$ and $P_2(t)$ depend not only on Δ^2, but also Δ. As a result, the latter shows nonreciprocal behavior but the former is reciprocal.

IV. CONCLUSION

We have investigated the controllable dissipation of a giant atom and its potential applications in a waveguide QED system. We showed that the decay rate of the giant atom can be well controlled by changing its size, that is, the distance between two points connecting with the waveguide. With state-of-the-art experimental feasibility, we proposed a robust entangled state preparation scheme. More interestingly, for a two-giant-atom setup, we found nonreciprocal excitation evolution for fixed atoms but reciprocal transmission between them.

We should point out that the controllable dissipation and effective interaction via tuning the size of the giant atom have also been studied in the waveguide with a linear dispersion relation [4,21]. In contrast, here we focused on a lattice waveguide model with a nonlinear dispersion relation [35]. The intersite coupling ξ, which modulates the group velocity of the photons in the waveguide ($v_g = \partial\omega_k/\partial k = 2\xi\sin k$), is also a sensitive parameter to control the dissipation and interaction [see Eqs. (6) and (11)]. Meanwhile, for our model, the waveguide forms an energy band and the non-Markovian effect will dominant when the atom is resonant with the edge of waveguide band in energy [36,37], which is not possible in the linear waveguide. The other origin of the non-Markovian effect comes from the time delay of the photon transmission [3,6] between the two connecting points, which may appear in the waveguide with both a linear and a nonlinear dispersion relation. However, these non-Markovian effects are beyond the scope of the present work.

In addition, the realization of the giant atom is limited not only in the photonic waveguide, but also in the acoustic system [38–41] and has been proposed theoretically in a cold-atom system [9]. Therefore, we hope that our investigation has potential application in quantum information processing in these physical systems.

ACKNOWLEDGMENTS

This work was supported by National Natural Science Foundation of China (Grants No. 11875011, No. 12047566, and No. 12074061).

APPENDIX A: MASTER EQUATION

In the main text we gave the final master equation for a single-giant-atom setup as Eq. (5); in this Appendix we will give some detailed derivations. Under the Markov approximation and working in the interaction picture, the formal master equation for a quantum open system reads [29]

$$\dot{\rho}(t) = -\int_0^\infty d\tau\, \mathrm{Tr}_c\{[H_I(t), [H_I(t-\tau), \rho_c \otimes \rho(t)]]\}. \tag{A1}$$

In our system, the interaction Hamiltonian is given in Eq. (3) and the master equation yields

$$\begin{aligned}\dot{\rho}(t) &= -\int_0^\infty d\tau\, \mathrm{Tr}_c\{[H_I(t), [H_I(t-\tau), \rho_c \otimes \rho(t)]]\} \\ &= -\int_0^\infty d\tau\, \mathrm{Tr}_c[H_I(t)H_I(t-\tau)\rho_c \otimes \rho(t)] + \int_0^\infty d\tau\, \mathrm{Tr}_c[H_I(t)\rho_c \otimes \rho(t)H_I(t-\tau)] \\ &\quad + \int_0^\infty d\tau\, \mathrm{Tr}_c[H_I(t-\tau)\rho_c \otimes \rho(t)H_I(t)] - \int_0^\infty d\tau\, \mathrm{Tr}_c[\rho_c \otimes \rho(t)H_I(t-\tau)H_I(t)].\end{aligned} \tag{A2}$$

Since we are working at zero temperature, the CRW is in the vacuum state initially. Therefore, we will have $\mathrm{Tr}_c[E^\dagger(n_i,t)E(n_j,t-\tau)\rho_c] = 0$ and Eq. (A2) becomes (returning to the Schrödinger picture)

$$\dot{\rho} = -i\Omega[|e\rangle\langle e|, \rho] + (A + A^*)\sigma^-\rho\sigma^+ - A\sigma^+\sigma^-\rho - A^*\rho\sigma^+\sigma^-, \tag{A3}$$

where [20]

$$
\begin{aligned}
A &= g^2 \int_0^\infty d\tau\, e^{i\Omega\tau} \mathrm{Tr}_c \\
&\quad \times \left(\sum_{i,j} E(n_i,t) E^+(n_j,t-\tau)\rho_c \right) \\
&= g^2 \sum_{i,j} \int_0^\infty d\tau\, e^{i\Omega\tau} \mathrm{Tr}[E(n_i,t)E^+(n_j,t-\tau)\rho_c] \\
&= g^2 \sum_{i,j} \int_0^\infty d\tau \frac{e^{i\Omega\tau}}{N_c} \\
&\quad \times \mathrm{Tr}\left(\sum_{k,k'} e^{-i\omega_k t} e^{ikn_i} a_k e^{i\omega_{k'}(t-\tau)} e^{-ik'n_j} a_{k'}^\dagger \rho_c \right) \\
&= g^2 \sum_{i,j} \int_0^\infty d\tau \frac{1}{N_c} \sum_k (e^{-i(\omega_k-\Omega)\tau} e^{-ik(n_j-n_i)}) \\
&= g^2 \sum_{i,j} \int_0^\infty d\tau \frac{1}{N_c} \sum_{n=0}^{N_c-1} e^{-i\Delta_c\tau} \\
&\quad \times e^{-2\pi i(n_j-n_i)n/N_c} e^{2i\xi\cos(2\pi/nN_c)\tau} \\
&= g^2 \sum_{i,j} \int_0^\infty d\tau \frac{e^{-i\Delta_c\tau}}{N_c} \sum_{n=0}^{N_c-1} e^{-2\pi i(n_j-n_i)n/N_c} \\
&\quad \times \sum_{m=-\infty}^{\infty} i^m J_m(2\xi\tau) e^{i2\pi nm/N_c} \\
&= g^2 \sum_{i,j} \int_0^\infty d\tau\, e^{-i\Delta_c\tau} i^{|n_i-n_j|} J_{|n_i-n_j|}(2\xi\tau) \\
&= g^2 \sum_{i,j} \frac{1}{2\xi} e^{i\pi|n_i-n_j|/2} \\
&= \frac{g^2}{\xi}(1+e^{i\pi|n_1-n_2|/2}). \qquad \text{(A4)}
\end{aligned}
$$

In the above calculations, we have considered that the giant atom is resonant with the bare cavity ($\Delta_c := \omega_c - \Omega = 0$) and we used the formula

$$
\int_0^\infty d\tau\, J_m(a\tau) = \frac{1}{|a|}. \qquad \text{(A5)}
$$

APPENDIX B: NUMERICAL SIMULATION OF A SINGLE-GIANT-ATOM SYSTEM

In this Appendix we will outline the procedure of the numerical simulation for the dissipation of a single giant atom. In the main text we derived analytically the master equation under the Markov approximation by considering the waveguide as a structured environment. The underlying physics behind the Markov approximation is that the environment loses its memory and remains in its initial state during the time evolution. Physically speaking, an excited giant atom will decay to the ground state with the emission of a photon. The emitted photon will then travel along the waveguide. To guarantee the validity of the Markov approximation, the emitted photon must leave the atomic regime and never return. To fulfill such a condition, we choose the atomic frequency to be resonant with the bare resonator such that the group velocity of the emitted photon achieves its maximum value, which makes the photon quickly leave the atom-waveguide connecting points. Meanwhile, we try to enlarge the length of the waveguide and induce a small decay for each resonator to stop the emitted photon from returning to the atomic regime. In the numerical simulation, we adopt a non-Hermitian manner by phenomenologically expressing the Hamiltonian as

$$
\begin{aligned}
H &= (\omega_c - i\kappa)\sum_j a_j^\dagger a_j - \xi \sum_j (a_j^\dagger a_{j+1} + \mathrm{H.c.}) \\
&\quad + \Omega|e\rangle\langle e| + g\left[\left(a_{n_1}^\dagger + a_{n_2}^\dagger\right)\sigma^- + \mathrm{H.c.}\right], \qquad \text{(B1)}
\end{aligned}
$$

where κ is the decay rate for each resonator in the waveguide. Then the excited amplitude of the giant atom is obtained numerically as

$$
P(t) = |\langle\psi(0)|e^{-iHt}|\psi(0)\rangle|^2, \qquad \text{(B2)}
$$

where $|\psi(0)\rangle = |e,G\rangle$ represents that the giant atom is in the excited state while all of the resonators in the waveguide are in their vacuum states. In the numerical simulation (see Fig. 2), we have chosen the length of the waveguide as $N_c = 4000$ and the decay rate for each resonator as $\kappa/\xi = 6\times10^{-3}$. We have also checked that for $N_c = 3000$–5000 and $\kappa/\xi = (3\times10^{-3})$–$(1.2\times10^{-2})$, the numerical results are nearly unchanged.

[1] T. Petroskya and S. Subbiaha, Physica E **19**, 230 (2003).
[2] A. Frisk Kockum, P. Delsing, and G. Johansson, Phys. Rev. A **90**, 013837 (2014).
[3] L. Guo, A. Grimsmo, A. F. Kockum, M. Pletyukhov, and G. Johansson, Phys. Rev. A **95**, 053821 (2017).
[4] A. F. Kockum, G. Johansson, and F. Nori, Phys. Rev. Lett. **120**, 140404 (2018).
[5] P. Türschmann, H. L. Jeannic, S. F. Simonsen, H. R. Haakha, S. Götzinger, V. Sandoghdar, P. Lodahl, and N. Rotenberg, Nanophotonics **8**, 1641 (2019).
[6] G. Andersson, B. Suri, L. Guo, T. Aref, and P. Delsing, Nat. Phys. **15**, 1123 (2019).
[7] A. González-Tudela, C. Sánchez Muñoz, and J. I. Cirac, Phys. Rev. Lett. **122**, 203603 (2019).
[8] L. Guo, A. F. Kockum, F. Marquardt, and G. Johansson, Phys. Rev. Research **2**, 043014 (2020).
[9] S. Guo, Y. Wang, T. Purdy, and J. Taylor, Phys. Rev. A **102**, 033706 (2020).
[10] B. Kannan *et al.*, Nature (London) **583**, 775 (2020).
[11] A. M. Vadiraj, A. Ask, T. G. McConkey, I. Nsanzineza, C. W. S. Chang, A. F. Kockum, and C. M. Wilson, Phys. Rev. A **103**, 023710 (2021).
[12] H. J. Kimble, Nature (London) **453**, 1023 (2008).
[13] J.-T. Shen and S. Fan, Phys. Rev. Lett. **95**, 213001 (2005).

[14] D. E. Chang, A. S. Sørensen, E. A. Demler, and M. D. Lukin, Nat. Phys. **3**, 807 (2007).
[15] P. Longo, P. Schmitteckert, and K. Busch, Phys. Rev. Lett. **104**, 023602 (2010).
[16] T. Shi, Y. Chang, and J. J. García-Ripoll, Phys. Rev. Lett. **120**, 153602 (2018).
[17] L. Zhou, Z. R. Gong, Y. X. Liu, C. P. Sun, and F. Nori, Phys. Rev. Lett. **101**, 100501 (2008).
[18] L. Zhou, L. P. Yang, Y. Li, and C. P. Sun, Phys. Rev. Lett. **111**, 103604 (2013).
[19] Z. H. Wang, L. Zhou, Y. Li, and C. P. Sun, Phys. Rev. A **89**, 053813 (2014).
[20] G. Calajó, F. Ciccarello, D. Chang, and P. Rabl, Phys. Rev. A **93**, 033833 (2016).
[21] H. Zheng and H. U. Baranger, Phys. Rev. Lett. **110**, 113601 (2013).
[22] E. Shahmoon and G. Kurizki, Phys. Rev. A **87**, 033831 (2013).
[23] P. Facchi, M. S. Kim, S. Pascazio, F. V. Pepe, D. Pomarico, and T. Tufarelli, Phys. Rev. A **94**, 043839 (2016).
[24] W. Zhao and Z. Wang, Phys. Rev. A **101**, 053855 (2020).
[25] D. W. Wang, H. T. Zhou, M. J. Guo, J. X. Zhang, J. Evers, and S. Y. Zhu, Phys. Rev. Lett. **110**, 093901 (2013).
[26] J.-H. Wu, M. Artoni, and G. C. La Rocca, Phys. Rev. Lett. **113**, 123004 (2014).
[27] B. Peng, S. K. Özdemir, F. Lei, F. Monifi, M. Gianfreda, G. L. Long, S. Fan, F. Nori, C. M. Bender, and L. Yang, Nat. Phys. **10**, 394 (2014).
[28] L. Chang, X. Jiang, S. Hua, C. Yang, J. Wen, L. Jiang, G. Li, G. Wang, and M. Xiao, Nat. Photon. **8**, 524 (2014).
[29] H. Breuer and F. Petruccione, *The Theory of Open Quantum Systems* (Oxford University Press, Oxford, 2002).
[30] S. Hacohen-Gourgy, V. V. Ramasesh, C. De Grandi, I. Siddiqi, and S. M. Girvin, Phys. Rev. Lett. **115**, 240501 (2015).
[31] P. Forn-Díaz, J. J. García-Ripoll, B. Peropadre, J.-L. Orgiazzi, M. A. Yurtalan, R. Belyansky, C. M. Wilson, and A. Lupascu, Nat. Phys. **13**, 39 (2017).
[32] F. Yoshihara, T. Fuse, S. Ashhab, K. Kakuyanagi, S. Saito, and K. Semba, Nat. Phys. **13**, 44 (2017).
[33] A. J. Keller, P. B. Dieterle, M. Fang, B. Berger, J. M. Fink, and O. Painter, Appl. Phys. Lett. **111**, 042603 (2017).
[34] J. J. Burnett, A. Bengtsson, M. Scigliuzzo, D. Niepce, M. Kudra, P. Delsing, and J. Bylander, npj Quantum Inf. **5**, 54 (2019).
[35] L. Zhou, H. Dong, Y.-x. Liu, C. P. Sun, and F. Nori, Phys. Rev. A **78**, 063827 (2008).
[36] I. de Vega, D. Alonso, and P. Gaspard, Phys. Rev. A **71**, 023812 (2005).
[37] I. de Vega and D. Alonso, Phys. Rev. A **77**, 043836 (2008).
[38] S. Datta, *Surface Acoustic Wave Devices* (Prentice-Hall, Englewood Cliffs, 1986).
[39] D. Morgan, *Surface Acoustic Wave Filters*, 2nd ed. (Academic, Amsterdam, 2007).
[40] M. V. Gustafsson, T. Aref, A. F. Kockum, M. K. Ekström, G. Johansson, and P. Delsing, Science **346**, 207 (2014).
[41] R. Manenti, A. F. Kockum, A. Patterson, T. Behrle, J. Rahamim, G. Tancredi, F. Nori, and P. J. Leek, Nat. Commun. **8**, 975 (2017).